

The twisted arc model for chiral molecules

Johannes Trost ^{*}, Klaus Hornberger

Arnold Sommerfeld Center for Theoretical Physics, Ludwig-Maximilians-Universität München, Theresienstraße 37, 80333 Munich, Germany

Received 2 February 2007; accepted 10 April 2007

Available online 20 April 2007

Abstract

We present a simple model for chiral molecules which yields the frequency-dependent multipole–multipole polarizabilities required for calculating the dispersive van der Waals constants in a simple, closed, and consistent form. The model consists of a single effective charge confined to a one-dimensional wire formed by two circular arcs, which are twisted with respect to each other by an angle characterizing the chirality. The resulting polarizabilities show a simple functional dependence on the model parameters, and they serve to mimic the chiral properties of small molecules, such as H_2S_2 , in a reasonably realistic way.

© 2007 Elsevier B.V. All rights reserved.

PACS: 33.15.Kr; 34.20.Gj; 33.55.Ad

Keywords: Chiral molecule; Twisted wire model; Multipole–multipole polarizability

1. Introduction

Wire models [1,2] are popular to describe molecular configurations where electrons are allowed to move almost freely along quasi-one-dimensional structures, as is the case e.g. with the dislocated π -electrons in organic chain molecules [3–5]. Studies comparing these models with ab initio electronic configuration calculations [2,6] show that, in spite of their simplicity, these models succeed in reproducing many qualitative features and yield even quantitatively reasonable results.

In the present article, we discuss a simple wire model which aims at describing small chiral molecules, and in particular the dependence of the chiral nature on their electronic susceptibilities. The latter determine important molecular properties such as the optical activity and the dispersion forces acting between molecules. While the chiroptical properties have already been subject of several publications [1–5], the present article is focused on the dispersion forces.

In general, it is a difficult task to calculate the dispersive interaction potential strengths between chiral molecules (with few or no symmetries) and other polarizable particles if one has to go beyond the bulk van der Waals force $U = -C_6/r^6$. This is the case, e.g. if one needs to assess the relative strength of chirality-discriminative part of the interaction versus the non-discriminative ones. The reason is that multipole–multipole polarizabilities are required on the whole imaginary frequency spectrum for calculating the higher order dispersion constants which are linear combinations of integrals [7]

$$\int_0^\infty \alpha_{m_A, m'_A}^{\ell_A, \ell'_A}(i\omega) \alpha_{m_B, m'_B}^{\ell_B, \ell'_B}(i\omega) d\omega, \quad (1)$$

where $\alpha_{m_A, m'_A}^{\ell_A, \ell'_A}$ and $\alpha_{m_B, m'_B}^{\ell_B, \ell'_B}$ denote the polarizabilities for molecules A and B, respectively, in spherical tensor notation, see Eq. (51).

The van der Waals dispersion constant C_6 depends on the electric-dipole–electric-dipole polarizabilities of both molecules ($\ell_A = \ell'_A = \ell_B = \ell'_B = 1$). While it does not discriminate between the left- and right-handed configurations of an oriented chiral molecule, higher order dispersion interactions differ in general for left and right

^{*} Corresponding author.

E-mail address: jtrost@theorie.physik.uni-muenchen.de (J. Trost).

configurations. Often, a rotational average over all orientations of the chiral molecule cancels this left-right distinction in the cross-sections. However, consider a coherent superposition of the left- and right-handed configuration states [8], which will be subject to decoherence due to collisions with the atoms of a surrounding gas. In this case, the decoherence process is determined by collisions of spherical gas atoms B off the oriented chiral molecule A . Here, the lowest order discriminative interaction with B ($\ell_B = \ell'_B = 1$) is given by the electric-dipole–electric-quadrupole polarizability [9], $\ell_A = 1$ and $\ell'_A = 2$. The resulting dispersive interaction depends on the distance r between the molecules as r^{-7} [10]. We will focus on this dominant discriminative interaction below, motivated by the above-mentioned question of collisional decoherence. We note that there might be additional forces of comparable strength which do not discriminate left and right, and that only non-retarded forces are considered in the following. For a discussion of retarded interaction between chiral molecules, see [11–13].

The main aim of the present model is therefore to provide a minimalist, while consistent and trustworthy model for the bulk electronic properties of chiral molecules. In particular, we give explicit and closed results for the rotatory power, the electric-dipole–electric-dipole polarizability, and the electric-dipole–electric-quadrupole polarizability, both at imaginary frequencies. The simplicity of the model even admits the calculation of further higher multipole–multipole polarizabilities with small effort.

The model is specified by two parameters, the length L determining the bulk polarizability and the twist angle χ , which corresponds to the dihedral angle in a molecule, see Fig. 1. By choosing the parameters to represent the chiral dihydrogen disulfide, H_2S_2 , we obtain reasonable values for its various electronic properties, suggesting that the model may serve as a good approximation for a typical small chiral molecule. Yet, the aim here is of course not to reproduce precise numbers, but to have an easily accessible, consistent and plausible description of the depen-

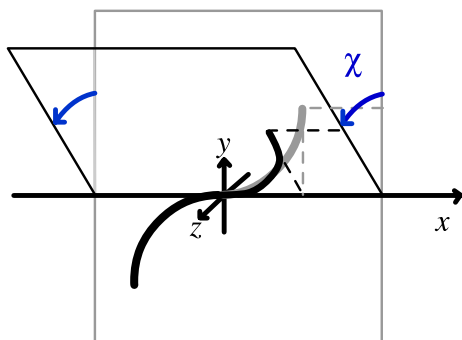


Fig. 1. The twisted arc model is given by a wire of length L in the form of two arcs formed by quarter circles. They can be twisted with respect to each other by an angle χ . This way a three-dimensional chiral structure is formed, except for $\chi = 0$ and $\chi = \pi$, when the wire is in its planar *trans*- and its *cis*-configuration.

dence of the electronic susceptibilities on the molecular parameters, and in particular on the dihedral angle.

The structure of the article is as follows. Section 2 presents the model and its quantization based on the canonical description of the one-dimensional dynamics. The explicit forms of the most important Cartesian operators (position, momentum, magnetic dipole, and electric quadrupole moment) are then derived in Section 3, together with closed expressions for their matrix elements in the energy eigenbasis. Based on these results the rotatory strength is calculated in Section 4, as a function of the chiral angle. Section 5 contains the calculation and discussion of the electric-dipole–electric-dipole and electric-dipole–electric-quadrupole polarizability for imaginary frequencies. An example for interaction strengths derived from the polarizabilities is discussed in Section 6 and we present our conclusions in Section 7.

2. The twisted arc model

Our model aims at describing the excitation properties of a chiral quantum system in the easiest possible way. It is formed by two connected circular arcs, \mathcal{C}_I and \mathcal{C}_{II} , each described by the common radius R and an angle of 90° . The total length of the wire is thus $L = \pi R$. We put the origin of the coordinate system at the junction of the arcs such that \mathcal{C}_I lies in the xy -plane. For $\chi = 0$ also \mathcal{C}_{II} lies in the xy -plane (*trans*-configuration), while for $\chi \neq 0$ it is turned around the x -axis, see Fig. 2. We call χ the twist angle, and take it as the angle between the osculating plane of \mathcal{C}_{II} and the y -axis ($-\pi < \chi \leq \pi$). For $\chi = \pi$ the wire is in its *cis*-configuration, and for $\chi \neq 0, \pi$ the angles χ and $-\chi$ correspond to configurations with opposite chirality. Alternatively one could choose the dihedral angle $\phi = \pi - \chi$.

A charged particle of mass M and charge q is confined to move freely along the wire defined by the two arcs. It is constrained by an infinite potential step at both ends, but there is no force in the x -direction at the joint of \mathcal{C}_I and \mathcal{C}_{II} .

The model shows C_2 symmetry. The symmetry axis (dashed line in Fig. 2) lies in the yz -plane and includes

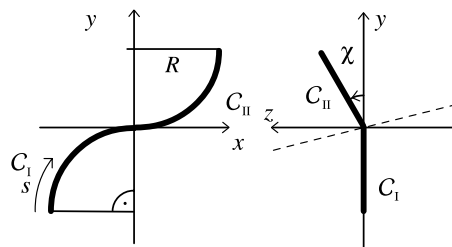


Fig. 2. Projections of the twisted wire model onto the xy -plane (left) and the yz -plane (right). The arcs \mathcal{C}_I and \mathcal{C}_{II} are quarter circles with a radius of $R = L/\pi$. \mathcal{C}_I lies in the xy -plane as indicated and the twist angle χ is defined to be positive (negative) for \mathcal{C}_{II} pointing into the positive (negative) z -direction. The origin of the parameterization coordinate s is taken to be the loose end of \mathcal{C}_I . The C_2 symmetry axis, drawn as a dashed line, lies in the yz -plane.

the origin. It has an angle of $-\chi/2$ with respect to the z -axis.

We note that an alternative construction, suggested in [5], would be to take (at least) three straight wire parts joint together at angles of 90° . We prefer the present cornerless structure, since it consists only of two equivalent legs which mirror the symmetry of the wave function, and admit simple closed expressions for the relevant matrix elements, see below. For a critical examination of the thin wire model with corners see [14]. Another widely used model for chiral molecules is the helical thin wire model [15], which, however, does not allow the straightforward modelling of the dihedral angle of H_2S_2 .

2.1. Quantization of the twisted arc

In order to quantize the motion let us first consider the canonical description of the classical motion [1]. The natural generalized coordinate is the length of the wire s ($0 \leq s \leq L$). Noting $R = L/\pi$ we find from Fig. 2 its relation to the Cartesian coordinates:

$$\begin{aligned} x &= -\frac{L}{\pi} \cos\left(\frac{\pi s}{L}\right), \\ y &= \begin{cases} \frac{L}{\pi} [\sin(\frac{\pi s}{L}) - 1] & \text{for } 0 \leq s \leq \frac{L}{2}, \\ \frac{L}{\pi} \cos \chi [1 - \sin(\frac{\pi s}{L})] & \text{for } \frac{L}{2} \leq s \leq L, \end{cases} \\ z &= \begin{cases} 0 & \text{for } 0 \leq s \leq \frac{L}{2}, \\ \frac{L}{\pi} \sin \chi [1 - \sin(\frac{\pi s}{L})] & \text{for } \frac{L}{2} \leq s \leq L. \end{cases} \end{aligned} \quad (2)$$

As can be easily checked, this parameterization guarantees that the kinetic energy T is given by the generalized velocity

$$T = \frac{M}{2} (\dot{x}^2 + \dot{y}^2 + \dot{z}^2) = \frac{M}{2} \dot{s}^2. \quad (3)$$

In the absence of a (magnetic) potential the Lagrange function equals the kinetic energy, $\mathcal{L} = T$. The conjugate momentum is defined as $p_s = \partial \mathcal{L} / \partial \dot{s} = M \dot{s}$, so that the Hamilton function $H = T$ takes the form $H = p_s^2 / (2M)$. The Cartesian components of the momentum are thus obtained, via $p_x = M \dot{x} = M (\partial x / \partial s) \dot{s}$, as

$$\begin{aligned} p_x &= \sin\left(\frac{\pi s}{L}\right) p_s, \\ p_y &= \begin{cases} \cos\left(\frac{\pi s}{L}\right) p_s & \text{for } 0 \leq s \leq \frac{L}{2}, \\ -\cos \chi \cos\left(\frac{\pi s}{L}\right) p_s & \text{for } \frac{L}{2} \leq s \leq L, \end{cases} \\ p_z &= \begin{cases} 0 & \text{for } 0 \leq s \leq \frac{L}{2}, \\ -\sin \chi \cos\left(\frac{\pi s}{L}\right) p_s & \text{for } \frac{L}{2} \leq s \leq L, \end{cases} \end{aligned} \quad (4)$$

We turn to the quantum description by replacing p_s by the differential operator

$$p_s = \frac{\hbar}{i} \frac{\partial}{\partial s}. \quad (5)$$

acting in $L_2([0, L])$. Operators will be indicated by sans-serifs throughout. The Hamiltonian is now

$$H = -\frac{\hbar^2}{2M} \frac{\partial^2}{\partial s^2}. \quad (6)$$

Together with the boundary condition $\psi(0) = \psi(L) = 0$, it yields the eigenfunctions of a particle in a one dimensional box with length L

$$\psi_n(s) = \sqrt{\frac{2}{L}} \sin\left(\frac{n\pi s}{L}\right), \quad n = 1, 2, 3, \dots \quad (7)$$

The corresponding energies depend quadratically on the excitation number, $E_n = n^2 E_1$, with the ground state energy given, for $M = m_e$, by

$$E_1 = \frac{\pi^2}{2} \left(\frac{L}{a_0}\right)^{-2} E_{\text{hartree}} = \frac{35.06 \text{ eV}}{(L/\text{\AA})^2}. \quad (8)$$

Choosing L as the sum of the binding lengths of H_2S_2 , i.e. $L = 8.6a_0$, yields a first excitation energy of $E_2 - E_1 = 3E_1 = 5.4 \text{ eV}$, which is in good agreement with the result of ab initio calculations for the excitation energy, 5.48 eV, for the longest wavelength transition [16].

In the following, we will use atomic units (a.u.), $\hbar = e_0 = m_e = 1$, with $M = m_e$.

3. The Cartesian operators

The functional dependence of the Cartesian operators on the coordinate s will in general be different on \mathcal{C}_I and \mathcal{C}_{II} . It is therefore convenient to introduce for any operator A the corresponding partial operators $A^{(I)}$ and $A^{(II)}$ satisfying

$$A(s) = \Theta\left(\frac{L}{2} - s\right) A^{(I)}(s) + \Theta\left(s - \frac{L}{2}\right) A^{(II)}(s). \quad (9)$$

The matrix elements of A with respect to the energy eigenstates (7) can then be calculated as

$$\begin{aligned} \langle m | A | n \rangle &= \int_0^{L/2} ds \psi_m^*(s) A^{(I)}(s) \psi_n(s) \\ &\quad + \int_{L/2}^L ds \psi_m^*(s) A^{(II)}(s) \psi_n(s). \end{aligned} \quad (10)$$

The C_2 symmetry of the wire model will allow to express matrix elements of operator A by the restricted operator $A^{(I)}$ alone, see below.

3.1. The position operator

The Cartesian dipole operator is determined by the Cartesian components of the position operator, $\vec{d} = q\vec{r}$. From (2) we obtain immediately

$$\begin{aligned} x^{(I)} &= -\frac{L}{\pi} \cos\left(\frac{\pi s}{L}\right) = x^{(II)}, \\ y^{(I)} &= \frac{L}{\pi} \left[\sin\left(\frac{\pi s}{L}\right) - 1 \right], \\ z^{(I)} &= 0, \end{aligned} \quad (11)$$

$$y^{(II)} = \frac{L}{\pi} \cos \chi \left[1 - \sin\left(\frac{\pi s}{L}\right) \right] = -\cos \chi y^{(I)},$$

$$z^{(II)} = \frac{L}{\pi} \sin \chi \left[1 - \sin\left(\frac{\pi s}{L}\right) \right].$$

As an advantage of the present model, the matrix elements can be shown to be simply interrelated

$$\begin{aligned}\langle m|z^{(\text{II})}|n\rangle &= (-)^{n+m+1} \sin \chi \langle m|y^{(\text{I})}|n\rangle, \\ \langle m|y^{(\text{II})}|n\rangle &= (-)^{n+m+1} \cos \chi \langle m|y^{(\text{I})}|n\rangle.\end{aligned}\quad (12)$$

It follows that only a small fraction of the matrix elements needs to be evaluated. For those we obtain

$$\begin{aligned}\langle m|x|n\rangle &= \langle m|x^{(\text{I})}|n\rangle + \langle m|x^{(\text{II})}|n\rangle \\ &= \begin{cases} -\frac{L}{2\pi}(\delta_{n,m+1} + \delta_{n,m-1}) & \text{for } m > 1, \\ -\frac{L}{2\pi}\delta_{n,2} & \text{for } m = 1, \end{cases} \\ \langle m|y^{(\text{I})}|n\rangle &= \frac{L}{\pi^2} \frac{1}{D_{mn}^2 - 2S_{mn} + 1} \left[\frac{2}{D_{mn}} (n(3m^2 + n^2 - 1))\gamma_n \sigma_m \right. \\ &\quad \left. - m(3n^2 + m^2 - 1)\gamma_m \sigma_n - 4mn \right] \\ &= \langle n|y^{(\text{I})}|m\rangle \quad \text{for } m \neq n, n \pm 1, \\ \langle 1|y^{(\text{I})}|n\rangle &= \begin{cases} -\frac{2L}{\pi^2} \frac{2D_{n1} + (S_{n1} + 1)\gamma_n}{nD_{n1}D_{n2}} & \text{for } n > 2, \\ -\frac{L}{3\pi^2} & \text{for } n = 2. \end{cases}\end{aligned}\quad (13)$$

Here we introduced abbreviations which will be used throughout the paper

$$\begin{aligned}S_{mn} &:= m^2 + n^2, \\ D_{mn} &:= m^2 - n^2.\end{aligned}\quad (14)$$

Moreover, the following factors show up frequently:

$$\gamma_m := \cos\left(\frac{m\pi}{2}\right) = \begin{cases} 1 & \text{for } m = 0 \bmod 4, \\ -1 & \text{for } m = 2 \bmod 4, \\ 0 & \text{otherwise;} \end{cases}\quad (15)$$

$$\sigma_m := \sin\left(\frac{m\pi}{2}\right) = \begin{cases} 1 & \text{for } m = 1 \bmod 4, \\ -1 & \text{for } m = 3 \bmod 4, \\ 0 & \text{otherwise.} \end{cases}\quad (16)$$

The matrix elements of dipole operators in spherical form are calculated from the basic matrix elements, Eq. (13)

$$\begin{aligned}\langle 1|d_0|n\rangle &= q\langle 1|z^{(\text{II})}|n\rangle = (-)^n \sin \chi q\langle 1|y^{(\text{I})}|n\rangle, \\ \langle 1|d_{\pm 1}|n\rangle &= \mp \frac{q}{\sqrt{2}} [\langle 1|x|n\rangle \pm i\langle 1|y|n\rangle] \\ &= \mp \frac{q}{\sqrt{2}} [\langle 1|x|n\rangle \pm i(1 - (-)^n \cos \chi)\langle 1|y^{(\text{I})}|n\rangle].\end{aligned}\quad (17)$$

3.2. The momentum operator

The Cartesian components of the momentum operator on the individual arcs can be obtained for the corresponding classical expressions (4). However, unlike the full operator \mathbf{p} , the hermiticity of $p^{(\text{I})}$ and $p^{(\text{II})}$ is not guaranteed.

By replacing the canonical momentum p_s in the symmetrized version of (4) by its corresponding operator (5), and carrying out the derivatives as far as possible, we get the Cartesian momentum operators

$$\begin{aligned}p_x^{(\text{I})} &= -i \left[\sin\left(\frac{\pi s}{L}\right) \frac{\partial}{\partial s} + \frac{\pi}{2L} \cos\left(\frac{\pi s}{L}\right) \right] = p_x^{(\text{II})}, \\ p_y^{(\text{I})} &= -i \left[\cos\left(\frac{\pi s}{L}\right) \frac{\partial}{\partial s} - \frac{\pi}{2L} \sin\left(\frac{\pi s}{L}\right) \right], \\ p_y^{(\text{II})} &= -i \cos \chi \left[-\cos\left(\frac{\pi s}{L}\right) \frac{\partial}{\partial s} + \frac{\pi}{2L} \sin\left(\frac{\pi s}{L}\right) \right] = -\cos \chi p_y^{(\text{I})}, \\ p_z^{(\text{I})} &= 0, \\ p_z^{(\text{II})} &= -i \sin \chi \left[-\cos\left(\frac{\pi s}{L}\right) \frac{\partial}{\partial s} + \frac{\pi}{2L} \sin\left(\frac{\pi s}{L}\right) \right] = -\sin \chi p_y^{(\text{I})}.\end{aligned}\quad (18)$$

The operators $p_y^{(\text{I})}$, $p_y^{(\text{II})}$, $p_z^{(\text{I})}$, and $p_z^{(\text{II})}$ are Hermitian, while $p_x^{(\text{I})}$ and $p_x^{(\text{II})}$, are individually not Hermitian, but only their sum. For example, $p_x^{(\text{I})}$ obeys the relation

$$\langle n|p_x^{(\text{I})}|m\rangle = \langle m|p_x^{(\text{I})}|n\rangle^* - \frac{2}{L} i s_n s_m.\quad (19)$$

The second term on the right-hand side is the boundary term of the partial integration showing up if the differential operator is applied to the bra. It does not necessarily vanish here, since the wave function may be finite at the boundary point $s = L/2$. A remedy would be to define a modified momentum operator

$$\tilde{p}_x^{(\text{I})} := p_x^{(\text{I})} + 2i\delta\left(s - \frac{L}{2}\right).\quad (20)$$

This operator on \mathcal{C}_I is now Hermitian, $\langle m|\tilde{p}_x^{(\text{I})}|n\rangle = \langle n|\tilde{p}_x^{(\text{I})}|m\rangle^*$, since the δ -function cancels the contribution of the boundary term. Similarly, the definition

$$\tilde{p}_x^{(\text{II})} := p_x^{(\text{II})} - 2i\delta\left(s - \frac{L}{2}\right)\quad (21)$$

ensures both the hermiticity on \mathcal{C}_{II} and the relation $p_x = \tilde{p}_x^{(\text{I})} + \tilde{p}_x^{(\text{II})}$. In general, it would be therefore more convenient to express momentum matrix elements in terms of the Hermitian operators (20) and (21). However, below the momentum operator will occur only as part of the magnetic dipole operator, where this modification is not required, as discussed next.

3.3. Magnetic dipole moments

The magnetic moment is proportional to the angular momentum operator

$$\vec{m} = q\vec{L} = q\vec{r} \times \vec{p} = q \begin{pmatrix} yp_z - zp_y \\ zp_x - xp_z \\ xp_y - yp_x \end{pmatrix},\quad (22)$$

where we still use atomic units and allow for an effective charge $q = Z_{\text{eff}}e_0$, which might be useful as a fitting parameter.

The magnetic dipole moment depends on the origin, and it is natural to choose the position of the joint between the two arcs in the present model. It can be easily seen that the non-hermiticity of the parts $p_x^{(\text{I})}$ and $p_x^{(\text{II})}$ is then irrelevant

since the x -component of the momentum is multiplied by y or z , which vanish at $s = L/2$ and thus suppress the hermiticity terms in Eqs. (20) and (21). The ability to evaluate the magnetic moment directly, without having to resort to Hermitian corrections, is another advantage of the present model.

Again one can derive helpful inter-relations of the matrix elements:

$$\begin{aligned} \langle m | (x p_y - y p_x)^{(II)} | n \rangle &= (-)^{n+m} \cos \chi \langle m | (x p_y - y p_x)^{(I)} | n \rangle, \\ \langle m | z p_x - x p_z | n \rangle &= \langle m | (z p_x - x p_z)^{(II)} | n \rangle \\ &= (-)^{n+m+1} \sin \chi \langle m | (x p_y - y p_x)^{(I)} | n \rangle, \\ \langle m | y p_z - z p_y | n \rangle &= \langle m | (y p_z - z p_y)^{(II)} | n \rangle = 0. \end{aligned} \quad (23)$$

The last relation follows immediately from the proportionality of y and z components of the operators and the vanishing of the z components on \mathcal{C}_1 . It follows that a single integral remains to be calculated.

$$i \langle m | (x p_y - y p_x)^{(I)} | n \rangle = \begin{cases} 0 & \text{for } n = m, \\ -\frac{4(4-\pi)m(m+1)-\pi}{8(2m+1)\pi} & \text{for } n = m + 1. \end{cases} \quad (24)$$

For $n > m + 1$ we get

$$\begin{aligned} i \langle m | (x p_y - y p_x)^{(I)} | n \rangle &= -[2mn(A_{mn}^2 - 1)(\Sigma_{mn}^2 - 1) + 2mn(2S_{mn} - 1)\gamma_m \gamma_n \\ &\quad + (2S_{mn}^2 - D_{mn}^2 - S_{mn})\sigma_m \sigma_n] / [\pi D_{mn}(A_{mn}^2 - 1)(\Sigma_{mn}^2 - 1)]. \end{aligned} \quad (25)$$

Here we added the abbreviations

$$\begin{aligned} \Sigma_{mn} &:= m + n \\ A_{mn} &:= m - n \end{aligned} \quad (26)$$

to those defined in (14)–(16). The hermiticity of the part $m_z^{(I)}$ is now evident, $\langle n | m_z^{(I)} | m \rangle = \langle m | m_z^{(I)} | n \rangle^*$, implying with (23) that all the components of \vec{m} are Hermitian.

3.4. Electric quadrupole moments

The quadrupole moments are given by a quadratic combination of the position operators. In Cartesian coordinates, $\vec{r} = (x, y, z)$, we have

$$Q_{ij} = q(3r_i r_j - \delta_{ik} r^2). \quad (27)$$

Again, a variety of proportionality relations serves to reduce the calculational effort considerably:

$$\begin{aligned} \langle n | y^{(II)2} | m \rangle &= \cos^2 \chi (-1)^{n+m} \langle n | y^{(I)2} | m \rangle, \\ \langle n | z^2 | m \rangle &= \langle n | z^{(II)2} | m \rangle \\ &= \sin^2 \chi (-1)^{n+m} \langle n | y^{(I)2} | m \rangle, \\ \langle n | x^{(II)} y^{(II)} | m \rangle &= \cos \chi (-1)^{n+m} \langle n | x^{(I)} y^{(I)} | m \rangle, \end{aligned}$$

$$\begin{aligned} \langle n | xz | m \rangle &= \langle n | x^{(II)} z^{(II)} | m \rangle \\ &= \sin \chi (-1)^{n+m} \langle n | x^{(I)} y^{(I)} | m \rangle, \\ \langle n | yz | m \rangle &= \langle n | y^{(II)} z^{(II)} | m \rangle \\ &= \sin \chi \cos \chi (-1)^{n+m} \langle n | y^{(I)2} | m \rangle. \end{aligned} \quad (28)$$

It follows that three integrals need to be evaluated:

$$\langle n | x^2 | m \rangle = \frac{L^2}{2\pi^2} \left(\delta_{mn} + \frac{1}{2} \delta_{m,n+2} + \frac{1}{2} s \delta_{m,n-2} \right), \quad (29)$$

$$\begin{aligned} \langle n | y^{(I)2} | m \rangle &= \frac{4L^2}{\pi^2} [2nm(A_{mn}^2 - 4)D_{mn} + 3n(5m^4 + n^4 + 10m^2n^2 \\ &\quad - 15m^2 - 5n^2 + 4)\gamma_n \sigma_m - 3m(5n^4 + m^4 + 10m^2n^2 \\ &\quad - 15n^2 - 5m^2 + 4)\gamma_m \sigma_n] \\ &\quad \times [D_{mn}(A_{mn}^2 - 4)(A_{mn}^2 - 1)(\Sigma_{mn}^2 - 4)(\Sigma_{mn}^2 - 1)]^{-1}, \end{aligned} \quad (30)$$

$$\begin{aligned} \langle n | x^{(I)} y^{(I)} | m \rangle &= \frac{2L^2}{\pi^3} [-2nm(A_{mn}^2 - 1)(\Sigma_{mn}^2 - 1) + 6mn(2S_{mn} - 5)\gamma_n \gamma_m \\ &\quad + 3(2S_{mn}^2 - D_{mn} - 5S_{mn} + 4)\sigma_n \sigma_m] \\ &\quad \times [(A_{mn}^2 - 4)(A_{mn}^2 - 1)(\Sigma_{mn}^2 - 4)(\Sigma_{mn}^2 - 1)]^{-1}. \end{aligned} \quad (31)$$

The last two expressions, (30) and (31), are valid for those combinations of values n and m for which the denominators do not vanish. We omit the general results for $m - n = 1, 2$ since the matrix elements will be needed only for $m = 1$ below. In this case they take the form:

$$\begin{aligned} \langle n | y^{(I)2} | 1 \rangle &= \frac{4L^2}{\pi^3 n D_{n,2}} \left(2 - \frac{3(n^2 + 6)\gamma_n}{D_{n,1} D_{n,3}} \right) \quad \text{for } n > 3, \\ \langle 2 | y^{(I)2} | 1 \rangle &= \frac{2L^2}{15\pi^3}, \\ \langle 3 | y^{(I)2} | 1 \rangle &= \frac{2L^2}{\pi^3} \left(\frac{4}{15} - \frac{\pi}{16} \right), \\ \langle n | x^{(I)} y^{(I)} | 1 \rangle &= \frac{2L^2}{\pi^3} \frac{2n D_{n,2} + 3S_{n,1} \sigma_n}{D_{n,1} D_{n,2} D_{n,3}} \quad \text{for } n > 3, \\ \langle 2 | x^{(I)} y^{(I)} | 1 \rangle &= \frac{4L^2}{\pi^3} \left(\frac{\pi}{16} - \frac{2}{15} \right), \\ \langle 3 | x^{(I)} y^{(I)} | 1 \rangle &= \frac{7L^2}{30\pi^3} \end{aligned} \quad (32)$$

Using these results one gets quite compact expressions for the quadrupole moments, which display a simple dependence on the twist angle χ . Here we note the matrix elements of the spherical quadrupole operators, $Q_{2,\mu}$, with magnetic quantum number μ . They are required for the calculation of the electric-dipole–electric-quadrupole polarizability in tensorial form, $\alpha_{k,k'}^{1,2}(\omega)$, see below:

$$\begin{aligned} \langle 1 | Q_{2,0} | n \rangle &:= \frac{q}{2} \langle 1 | 2z^2 - x^2 - y^2 | n \rangle \\ &= -\frac{q}{2} \langle 1 | x^{(I)2} | n \rangle - \frac{q}{2} [(-1)^n (3 \sin^2 \chi - 1) + 1] \langle 1 | y^{(I)2} | n \rangle, \end{aligned}$$

$$\begin{aligned}
\langle 1|Q_{2,\pm 1}|n\rangle &:= \mp q\sqrt{\frac{3}{2}}\langle 1|zx \pm izy|n\rangle \\
&= \pm q\sqrt{\frac{3}{2}}\sin\chi(-1)^n(\langle 1|x^{(1)}y^{(1)}|n\rangle \pm i\cos\chi\langle 1|y^{(1)2}|n\rangle), \\
\langle 1|Q_{2,\pm 2}|n\rangle &:= q\sqrt{\frac{3}{8}}\langle 1|x^2 \pm 2ixy - y^2|n\rangle \\
&= q\sqrt{\frac{3}{8}}\{\langle 1|x^{(1)2}|n\rangle \pm 2i[1 - (-1)^n\cos\chi]\langle 1|x^{(1)}y^{(1)}|n\rangle \\
&\quad - [1 - (-1)^n\cos^2\chi]\langle 1|y^{(1)2}|n\rangle\}. \tag{33}
\end{aligned}$$

4. The rotatory strength

We proceed with the discussion of the rotatory strength, the most prominent property of chiral molecules. We do so to demonstrate the ability of the twisted arc model to display electromagnetic properties of real, chiral molecules. The latter are usually optically active, and their chiroptical properties depend on the optical rotatory tensor [17]:

$$R_{ij}^{n1} = \text{Im}\{\langle 1|d_i|n\rangle\langle n|m_j|1\rangle\}. \tag{34}$$

The trace of the optical rotatory tensor yields the rotatory strength

$$R^{n1} = R_{xx}^{n1} + R_{yy}^{n1} + R_{zz}^{n1} = \text{Im}\{\langle 1|\vec{d}|n\rangle \cdot \langle n|\vec{m}|1\rangle\}. \tag{35}$$

It determines the optical rotation angle for orientationally averaged molecules. Recognizing an energy-resolution of the identity operator one finds that the sum over all states must vanish

$$\sum_{n=1}^{\infty} R^{n1} = \text{Im}\sum_{n=1}^{\infty} \langle 1|\vec{d}|n\rangle \cdot \langle n|\vec{m}|1\rangle = \text{Im}\langle 1|\vec{d} \cdot \vec{m}|1\rangle = 0, \tag{36}$$

because the expectation value of the Hermitian operator $\vec{d} \cdot \vec{m}$ must be real. We note also that the rotatory strength does not depend on the choice of origin. The most convenient choice of origin is therefore the joint of the arcs, since hermiticity corrections of the momentum operator are then not required, as discussed above. Note that an object independent of the origin is obtained by amending the rotatory tensor (34) with additional terms depending on the quadrupole–dipole tensor, which, however, cancel out after rotational averaging [18].

From the above formulas for the matrix elements of \vec{m} and \vec{d} one obtains

$$\begin{aligned}
R^{n1} &= Z_{\text{eff}}^2 L \frac{4}{\pi^3} \sin\chi(-1)^n \\
&\quad \times \left[\frac{4}{D_{n,1}D_{n,2}} + \frac{2(n^2+2)\gamma_n}{D_{n,1}^2D_{n,2}} + \frac{2(n^2+5)\sigma_n}{nD_{n,1}D_{n,2}^2} \right] \quad \text{for } n > 2, \tag{37}
\end{aligned}$$

$$R^{21} = Z_{\text{eff}}^2 L \frac{4}{3\pi^3} \sin\chi \left(\frac{2}{3} - \frac{3\pi}{16} \right). \tag{38}$$

As one expects, the rotatory strength is antisymmetric with respect to the twist angle, and the sum rule (36) for the rotatory strength is fulfilled.

Reasonable parameters for a small chiral molecule such as for H_2S_2 are $L = 8.6$ and $Z_{\text{eff}}^2 = 4.5$ (see Section 5.2). With these values one finds that R^{21} for $\chi = \frac{\pi}{2}$ is 0.388 a.u., corresponding to about 180×10^{-40} esu, which is larger by a factor of 5–10 compared with theoretical values for H_2S_2 [16,19]. This is mainly due to cancellation effects generated by the two lowest lying excited states of H_2S_2 , which are nearly degenerated for dihedral angles around $\pi/2$. They have rotatory strengths which are similar in absolute values but opposite in sign [16].

Having found reasonable choices for the parameters L and Z_{eff} , we now proceed to evaluate the frequency dependent rotatory power $G'(\omega)$, a further quantity which permits a comparison with the literature values of the real molecule H_2S_2 . The rotatory power is expressed by the electric-dipole–magnetic-dipole polarizability [20]:

$$G'_{ij}(\omega) = -2\omega \sum_{n=2}^{\infty} \frac{R_{ij}^{n1}}{(E_n - E_1)^2 - \omega^2}. \tag{39}$$

The average over all orientations of G'_{ij} is given by the trace

$$G'(\omega) = \sum_{i=x,y,z} G'_{ii}(\omega) = -2\omega \sum_{n=2}^{\infty} \frac{R^{n1}}{(E_n - E_1)^2 - \omega^2}, \tag{40}$$

which can be expanded for small frequencies (compared to the excitation gap). For $\chi = \pi/2$ we find

$$G'_{\pi/2}(\omega)Z_{\text{eff}}^2L^{-3} = -1.142 \times 10^{-4}\omega - 1.61 \times 10^{-5}\omega^3 + \text{O}(\omega^5). \tag{41}$$

Here, the frequencies are in units of E_1/\hbar . The polarizability, given in atomic units, scales as $Z_{\text{eff}}^2L^3$, where a factor Z_{eff}^2L is contributed by the dimensions of the rotatory tensor and a factor L^2 by the decrease of the excitation energy with increasing length scale.

The specific rotation angle ϕ per dm can be calculated as (see e.g. [10])

$$\phi(\omega) = -187.5^\circ \text{ dm}^{-1} \sin\chi \frac{\eta}{(\text{mol/dl})} \frac{\hbar\omega}{E_1} G'_{\pi/2} \left(\frac{\hbar\omega}{E_1} \right), \tag{42}$$

where η is the concentration of chiral molecules modeled by twisted wires. The validity of (42) is restricted to frequencies well below the first excitation energy. Inserting the frequency for the sodium D-line ($E_{\text{Na}} \approx 1.17E_1$ for $L = 8.6a_0$), with the above choice of $L = 8.6a_0$ and $Z_{\text{eff}}^2 = 4.5$, one gets

$$\phi_{\text{Na-D}} = -103^\circ \text{ dm}^{-1} \sin\chi \frac{\eta}{(\text{mol/dl})}. \tag{43}$$

The specific rotation angle of H_2S_2 has a somewhat different functional dependency on χ due to above-mentioned cancellation effects, but its value is about the same order of magnitude as in CI calculations [19].

Note that the optical rotatory tensor (34) appears in the discriminatory part of the dispersion interaction between

two chiral molecules (here without rotational averaging) [17]:

$$E_{\text{ch-ch}} = \frac{2}{R^6} \left(\delta_{ik} - 3\widehat{R}_i\widehat{R}_k \right) \left(\delta_{jl} - 3\widehat{R}_j\widehat{R}_l \right) \sum_{n,m} \frac{R_{ij}^{n1} R_{kl}^{m1}}{E_{n1} + E_{m1}}. \quad (44)$$

We will not evaluate the expression further since we are mainly concerned with interactions between a chiral molecule and achiral atoms.

5. Electric multipole–multipole polarizabilities

We proceed to calculate the electric multipole–multipole polarizability tensor required for evaluating the dispersion interaction coefficients, C_6 and C_7 . With this application in mind, the results will not be presented in full generality, but

$$\alpha(i\omega, \chi) = Z_{\text{eff}}^2 L^4 \begin{pmatrix} a(\omega) & \frac{2}{3\pi}(1+c_\chi)a(\omega) & \frac{2}{3\pi}s_\chi a(\omega) \\ \frac{2}{3\pi}(1+c_\chi)a(\omega) & g_+(\omega)(1+c_\chi^2) + 2g_-(\omega)c_\chi & (g_+(\omega) + g_-(\omega)c_\chi)s_\chi \\ \frac{1}{3\pi}s_\chi a(\omega) & (g_+(\omega) + g_-(\omega)c_\chi)s_\chi & g_+(\omega)s_\chi^2 \end{pmatrix} \quad (49)$$

will be confined to the ground state polarizability at imaginary frequencies.

5.1. General form of the electric-dipole–electric-dipole polarizability tensor

Apart from α_{xx} , all elements of the polarizability tensor α depend on the twist angle χ . We start by discussing this dependence in more detail, noting that the elements of the polarization tensor of the state m are given as [20]

$$\alpha_{ij}^{(m)}(\omega, \chi) = \sum_{n \neq m} \left[\frac{\langle m | d_i(\chi) | n \rangle \langle n | d_j(\chi) | m \rangle}{E_n - E_m - \omega} + \frac{\langle m | d_j(\chi) | n \rangle \langle n | d_i(\chi) | m \rangle}{E_n - E_m + \omega} \right], \quad (45)$$

where $i, j \in \{x, y, z\}$.

Due to the time-reversal invariance the tensor elements are real at imaginary frequencies, see e.g. [21], implying that the tensor is a symmetric matrix and can hence be written as

$$\alpha_{ij}^{(m)}(i\omega, \chi) = 2 \sum_{n \neq m} \frac{(E_n - E_m)}{(E_n - E_m)^2 + \omega^2} \langle m | d_i(\chi) | n \rangle \langle n | d_j(\chi) | m \rangle. \quad (46)$$

For the special case $m = 1$ and inserting $\vec{d} = Z_{\text{eff}}\vec{r}$ we get finally

$$\alpha_{ij}^{(1)}(i\omega, \chi) = \frac{4L^2 Z_{\text{eff}}^2}{\pi^2} \sum_{n=2}^{\infty} \frac{(n^2 - 1) \langle 1 | r_i(\chi) | n \rangle \langle n | r_j(\chi) | 1 \rangle}{(n^2 - 1)^2 + \omega^2}, \quad (47)$$

where we absorbed a factor $\pi^2/2L^2$ into the frequency, thus measuring the frequency ω again in units of E_1/\hbar , see (8).

The index indicating the reference state $m = 1$ will be suppressed from now on.

We find that, due to the interrelations of the position matrix elements noted above, the frequency dependence of the spherical tensor is determined by only three functions:

$$\begin{aligned} g_e(\omega) &= \frac{4}{\pi^2 L^2} \sum_{n=2,4,\dots} \frac{n^2 - 1}{(n^2 - 1)^2 + \omega^2} \langle n | y^{(1)} | 1 \rangle^2, \\ g_o(\omega) &= \frac{4}{\pi^2 L^2} \sum_{n=3,5,\dots} \frac{n^2 - 1}{(n^2 - 1)^2 + \omega^2} \langle n | y^{(1)} | 1 \rangle^2, \\ a(\omega) &= \frac{1}{\pi^4} \frac{3}{9 + \omega^2}. \end{aligned} \quad (48)$$

With their help the structure of α at imaginary frequencies is readily specified

Here we used the abbreviations $s_\chi := \sin\chi$ and $c_\chi := \cos\chi$ and $g_\pm(\omega) := g_e(\omega) \pm g_o(\omega)$. The sums in (48) converge rapidly as the terms are of order $O(n^{-6})$ for large n .

The dependence on the twist angle is particularly simple in (49) due to the proportionality relations (12). One observes that only the off-diagonal elements in the third row and the third column change their sign when switching to opposite handedness, $\chi \rightarrow -\chi$. Such a change of sign in χ is equivalent to a reflection at the xy -plane, $z \rightarrow -z$. After an additional rotation by π around the z -axis a full parity operation, $\vec{r} \rightarrow -\vec{r}$, is obtained. Hence, one gets the tensor of the $-\chi$ configuration after rotating the polarizability tensor of the $+\chi$ configuration, which illustrates the well known fact that all dispersive interactions solely derived from the electric-dipole–electric-dipole polarizability tensor do not discriminate left- and right-handed enantiomers.

5.2. Choice of parameters

In the following we present numerical results for a specific choice of parameters, which are adapted to mimic the literature values for H_2S_2 , e.g. [16,19]. First we fix the length parameter L by the sum of the binding lengths of the molecule which is found to be $8.6a_0$. The twist angle in the wire model is chosen to be $\chi = \pm \frac{\pi}{2}$ which is a good approximation of the dihedral angle in the molecule.

To fix the effective charge Z_{eff} we consider the static (i.e., $\omega = 0$) values for the electric-dipole–electric-dipole polarizability $g_+(0) = 1.963 \times 10^{-4}$ a.u., $g_-(0) = 1.218 \times 10^{-4}$ a.u., and $a(0) = 3.42 \times 10^{-3}$ a.u. The values of g_+ and g_- as function of ω are depicted in Fig. 3. A comparison with the Lorentzian $Z_{\text{eff}}^2 L^4 a(\omega)$ from (48), which has a width

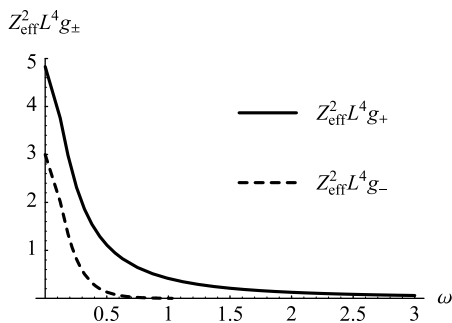


Fig. 3. Frequency dependence of the functions $Z_{\text{eff}}^2 L^4 g_+(\omega)$ (solid line) and $Z_{\text{eff}}^2 L^4 g_-(\omega)$ (dashed line) [atomic units; $L = 8.6$; $Z_{\text{eff}}^2 = 4.5$]. The frequency is given in terms of the ground state energy E_1/\hbar , see (8).

of 3 and a strength of 84.2, shows that the latter dominates the polarizability tensor.

The rotational average of the static polarizability for $\chi = \pm \pi/2$ is then given by

$$L^4 Z_{\text{eff}}^2 \bar{\alpha}(0) = \frac{L^4 Z_{\text{eff}}^2}{3} (\alpha_{xx}(0) + \alpha_{yy}(0) + \alpha_{zz}(0)) \approx L^4 Z_{\text{eff}}^2 1.271 \times 10^{-3} \text{ a.u.} \quad (50)$$

Here the contribution of $\alpha_{xx}(0)$ dominates the average static polarizability. A comparison with the literature value [16] for H_2S_2 of about 31 a.u. results in $Z_{\text{eff}}^2 = 4.5$ ($Z_{\text{eff}} \approx 2.12$).

5.3. Electric-dipole–electric-quadrupole polarizability

The dominant discriminative dispersion interaction between an oriented chiral and an achiral atom or molecule depends on the electric-dipole–electric-quadrupole polarizability tensor [9]. In addition to the dipole matrix elements, it is determined by the matrix elements quadratic in the coordinate operators, $\langle n|r_i r_j|m\rangle$, discussed in Section 3.4.

For the calculation of dispersion constants it is preferable to consider polarizability tensors for imaginary frequencies in spherical representation

$$\alpha_{k,k'}^{\ell,\ell'}(i\omega) = \frac{1}{2\pi} \sqrt{(2\ell+1)(2\ell'+1)} \times \sum_{n=2}^{\infty} \frac{E_n - E_1}{(E_n - E_1)^2 - (i\omega)^2} \langle 1|Q_{\ell,k}|n\rangle \langle n|Q_{\ell',k'}|1\rangle, \quad (51)$$

with the spherical multipole functions

$$Q_{\ell,k}(\vec{r}) = Z_{\text{eff}} r^\ell \sqrt{\frac{4\pi}{2\ell+1}} Y_{\ell,k}(\theta, \varphi). \quad (52)$$

For the electric-dipole–electric-quadrupole polarizability the multipole operators have ranks $\ell = 1$ and $\ell' = 2$,

$$\alpha_{k,k'}^{1,2}(i\omega) = \frac{\sqrt{15}}{2\pi} \sum_{n=2}^{\infty} \frac{E_n - E_1}{(E_n - E_1)^2 + \omega^2} \langle 1|d_k|n\rangle \langle n|Q_{2,k'}|1\rangle. \quad (53)$$

The required matrix elements can be found in (17) and (33). Obviously, the polarizability $\alpha_{k,k'}^{1,2}$ transforms under parity operation like a product of three coordinates, $r_i r_j r_k$, which results in an overall negative sign. Thus, the dispersive interaction derived from it discriminates left-handed and right-handed molecules. Finally, it should be noted that the electric-dipole–electric-dipole polarizability $\alpha^{1,1}$ does not depend on the choice of the origin, while the electric-quadrupole–electric-dipole polarizability $\alpha^{2,1}$ does [10].

6. Potential strengths

As an illustration for the use of the polarizability tensors, let us evaluate the interaction potential between a helium atom in ground state and the twisted arc. Its calculation requires the electric-dipole–electric-dipole polarizability of helium. Since helium is spherically symmetric only a single element of the spherical polarizability tensor does not vanish, namely $\alpha_{0,0}^{1,1}$. For our purposes it suffices to approximate the helium polarizability by

$$\alpha_{0,0}^{1,1}(i\omega) = \frac{g}{\omega_{\text{He}}^2 + \omega^2} \quad (54)$$

with $g = 2$ and $\omega_{\text{He}} \approx 1.33$ (atomic units), which is a good approximation for frequencies well below the excitation energy [22].

After evaluating the integrals (1) the dispersion potentials can be calculated following the theory in [23] by disregarding retardation effects. They assume the form

$$U_6(\vec{r}) = -\frac{C_6(\hat{r})}{r^6} \quad \text{and} \quad U_7(\vec{r}) = -\frac{C_7(\hat{r})}{r^7} \quad (55)$$

with \vec{r} the distance vector between helium atom and the center of mass, and $\hat{r} = \vec{r}/r$. For simplicity, we take the center of mass to lie in the origin. The potential strength $C_6(\hat{r})$ is calculated using the spherical dipole–dipole polarizability tensor, $\alpha_{kk'}^{1,1}$, of the twisted wire model which is readily obtained from the Cartesian polarizability (49). The calculation of $C_7(\hat{r})$ uses the dipole–quadrupole tensor (53).

To compare the interaction potentials we consider the surface of equality:

$$r_{\text{eq}}(\hat{r}) = \frac{|C_7(\hat{r})|}{|C_6(\hat{r})|}. \quad (56)$$

Thus, at distances $r = \xi r_{\text{eq}}$ the strengths of the potentials are related by $|U_6| = \xi |U_7|$. Since the potential strengths are linear combinations of the polarizabilities $r_{\text{eq}}(\hat{r})$ is proportional to L . At the same time, the dependence on Z_{eff} cancels out.

Fig. 4 shows C_7/C_6 for twist angles $\chi = \pi$ and $\chi = \pm\pi/2$ at $L = 8.6a_0$. Here, the direction of the helium atom, $\hat{r} = (\theta, \varphi)$, is specified with respect to the symmetry axis of the twisted wire (the dashed line in Fig. 2). The azimuthal angle (with respect to the x -axis) is chosen to be $\varphi = \pi/2$. Negative values of C_7/C_6 indicate that $U_7(\vec{r})$ is repulsive. As can be seen, the achiral *cis*-configuration $\chi = \pi$ is anti-symmetric with respect to $\theta = \pi/2$ (dash-

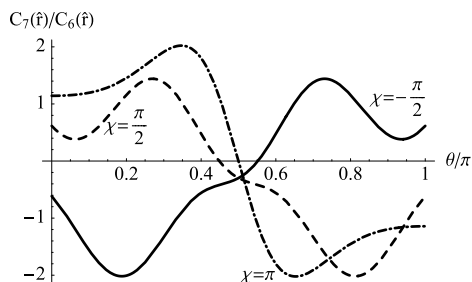


Fig. 4. The relative strength of the discriminative potential $C_7(\hat{r})$ compared to the dipole–dipole potential $C_6(\hat{r})$ in Bohr radii as a function of the polar angle θ (see text). The azimuthal angle is chosen to be $\varphi = \frac{\pi}{2}$ and the values of the three different twist angles χ are indicated in the figure.

dotted line). This is the case for all φ , and it is a consequence of the additional reflection symmetry for a planar configuration. For the other achiral situation, $\chi = 0$ (the *trans*-configuration), the potential strength C_7 vanishes identically, $C_7 = 0$. For all pairs of left- and right-handed configurations, $\chi \neq 0, \pi$, the surfaces of equality cannot be transformed into each other by a proper rotation. Thus, unlike U_6 , the U_7 interaction does distinguish between right- and left-handed form, the difference depending on both the distance $r = \zeta r_{\text{eq}}$, and the orientation \hat{r} .

7. Conclusions

We described a minimalist model for chiral molecules, which, in spite of its simplicity, admits a physically plausible and consistent description of their chiral properties. As a big advantage of this twisted arc model, the evaluation of higher order electric moments can be reduced to a small number of simple functions given in closed form. This way the functional dependence of the multipole polarizabilities on the frequency and on the model parameters shows up transparently. The derived chiral properties, such as the rotatory strength and the dispersive interaction potentials, thus display a simple, while physically consistent dependence on the model parameters. This was demonstrated, specifically for the dihedral angle, by evaluating the chirality-distinguishing part of the dispersive interaction with a

polarizable atom for molecular parameters adopted to the dihydrogen disulfide molecule. The comparison with the dominant bulk interaction thus permits to assess to what degree right- and left-handed, oriented molecules can be distinguished by the dispersion interaction.

Acknowledgement

This work was supported by the Emmy Noether program of the DFG.

References

- [1] I. Tinoco, R. Woody, *J. Chem. Phys.* 40 (1964) 160.
- [2] H.J. Nolte, V. Buss, *Tetrahedron* 31 (1975) 719.
- [3] N.L. Balazs, T.R. Brocki, I. Tobias, *Chem. Phys.* 13 (1976) 141.
- [4] E. Leuliette-Devin, R. Locqueneux, J. Tillieu, *J. Chem. Phys.* 75 (1981) 1239.
- [5] R.K. Kondru, S. Lim, P. Wipf, D.N. Beratan, *Chirality* 9 (1997) 469.
- [6] E.A. Power, T. Thirunamachandran, *Chem. Phys. Lett.* 3 (1969) 361.
- [7] W. Rijks, P.E.S. Wormer, *J. Chem. Phys.* 90 (1989) 6507.
- [8] J.A. Cina, R.A. Harris, *Science* 267 (1995) 832.
- [9] Y.N. Chiu, A.V. Kenney, S.H. Brown, *J. Chem. Phys.* 73 (1980) 1422.
- [10] A.J. Stone, *The Theory of Intermolecular Forces*, Clarendon Press, Oxford, 1996.
- [11] C. Mavroyannis, M.J. Stephen, *Mol. Phys.* 5 (1962) 629.
- [12] J.K. Jenkins, A. Salam, T. Thirunamachandran, *Phys. Rev. A* 50 (1994) 4767.
- [13] D.P. Craig, T. Thirunamachandran, *Theor. Chem. Acc.* 102 (1999) 112.
- [14] E.A. Power, T. Thirunamachandran, *Proc. Roy. Soc. Ser. A* 313 (1969) 403.
- [15] D.N. Sears, C.J. Jameson, R.A. Harris, *J. Chem. Phys.* 119 (2003) 2694.
- [16] A. Rauk, *J. Am. Chem. Soc.* 106 (1984) 6517.
- [17] D.P. Craig, T. Thirunamachandran, *Molecular Quantum Electrodynamics*, Academic Press, London, 1984.
- [18] A.D. Buckingham, M.B. Dunn, *J. Chem. Soc. (A)* (1971) 1988.
- [19] M. Pericou-Cayere, M. Rerat, A. Dargelos, *Chem. Phys.* 226 (1998) 297.
- [20] A.D. Buckingham, in: J.O. Hirschfelder (Ed.), *Permanent and Induced Molecular Moments and Long-Range Intermolecular Forces*, Intermolecular Forces, Wiley, New York, 1967.
- [21] L.D. Landau, E.M. Lifschitz, *Quantenmechanik*, Akademie Verlag, Berlin, 1988.
- [22] Y.M. Chan, A. Dalgarno, *Proc. Phys. Soc.* 86 (1965) 777.
- [23] V.P. Osinga, S.J.A. van Gisbergen, J.G. Snijders, E.J. Baerends, *J. Chem. Phys.* 106 (1997) 5091.